Fabrication of self-organized copper nanostructures on structureless surfaces

R. Kunz*, L. Kipp**, M. Skibowski**, R. Adelung*

*Chair for Multicomponent Materials, Faculty of Engineering,
University of Kiel, Germany, ra@tf.uni-kiel.de
**Institut for Experimental and Applied Physics, University of Kiel, Germany

ABSTRACT

An easy way to cover large areas with nano- or microstructures is self-organization. Against intuition, we claim that structureless crystals, in terms of surface features, are well-suited for self-organized structuring on the nano- and micrometer scale. We show examples of various structures obtained after copper evaporation on the flat surfaces of layered crystals. The structures found range from 8 nm thick nanowires [1] covering in a network with mesh diameters of 200-400 nm crystals on the millimeter scale, geometric figures in the micron range, to tunnel networks with diameter of 2-3 μm and mesh width of up to 100 μm. These structures grow because, These structures form due to two competing mechanisms; Long diffusion lengths enable a long-range organization, and weak substrate-absorbate interaction enables more complex phenomena to determine the structure. In contrast to a simple "stick if reached place" mechanism of surfaces with pronounced adsorption energy differences, here more complex "second order" phenomena such as strain, charge transfer, and differences in diffusion speed dictate the structures.

Keywords: copper, nanowire network, layered crystal, structuring, self organization.

1 INTRODUCTION

Layered transition-metal dichalcogenides (TMDC) have been the subject of many experimental and theoretical investigations[2–5]. They have been extensively studied since circa 1970. This is mainly due to their quasi-two-dimensionality and resulting unique physical properties. The low dimensionality results from the crystal structure: the TX_2 (T=transition-metal, X=chalcogen-atom) substrate consists of two-dimensional X-T-X sandwiches in either 1T or 2H coordination, separated by a van der Waals gap (Figure 1). The material will easily cleave along this gap, producing well-ordered surfaces. These surfaces exhibit extremely low defect densities, exhibiting no dangling bonds and no step edges for regions larger than $100\mu m^2$. TMDCs are of technological interest as intercalation compounds for batteries, as solar cell materials (the semiconductors WSe_2 or MoS_2) or simply as high tech lubricants (e.g. MoS_2). They can be produced as flakes via chemical vapor transport growth process as of up to 1 cm^2.

Surprisingly, there were not many experiments performed looking at the surfaces after evaporation of metals in ultra high vacuum. Otherwise, it would have be discovered earlier than in 1998, that a simple evaporation of certain metals in UHV leads to the formation of nanowire networks in a self organized process on the flat surfaces. First, it was discovered that the deposition of the alkali metal Rb leads to a formation of nanowire networks on many TMDCs (e.g. $TiTe_2$, TaS_2, VSe_2, WSe_2, TiS_2, $NbSe_2$). Because TMDCs can be metallic as well as semiconducting, some electronic properties could be modified [6-7], but due to the nature of the alkali metal these structures were not stable in air. Later it could be shown that copper will also form nanowires [1], but so far known only on VSe_2 and $TiSe_2$.

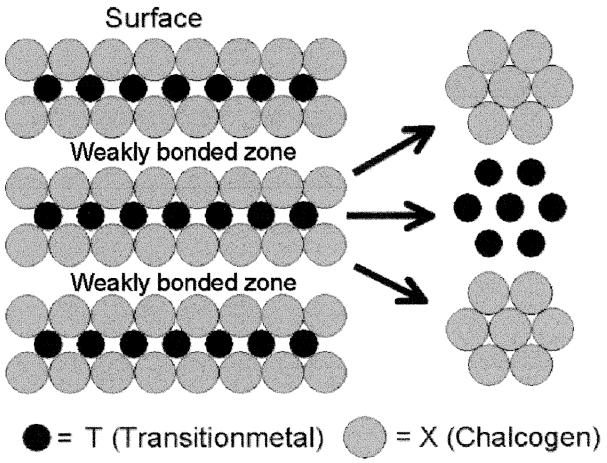

Figure 1: Schematic cut through a layered crystal

A systematic study was undertaken to determine why nanowire networks formed after copper evaporation do not form on crystals other than VSe_2 and $TiSe_2$,. This experiments yielded many different patterns self-organizing on the layered crystal surface. This is contrary to presently-used methods to create nanostructures on pre-structured surfaces. Typical examples of pre-structured surfaces are reconstructed or vicinal surfaces (e.g., stepped silicon) [8].

2 EXPERIMENTAL

The TMDC crystals, which included VSe_2, TaS_2, $TiTe_2$, TiS_2 and WSe_2, were fabricated with a chemical vapor

transport growth process. All surfaces were cleaved before metal evaporation, either directly in the vacuum or in air. Evaporation was carried out in UHV, with a background pressure in the low 10^{-10} mbar range for in-vacuum cleaved crystals or with a base pressure of $5*10^{-8}$ mbar for air-cleaved samples. The evaporations lead to 5-10nm copper thickness. The air-cleaved crystals were exposed to the copper at the same time ensuring the same preparation conditions.

The vacuum-cleaved surfaces were studied in a connected vacuum chamber with a scanning tunneling microscope (STM). The other sample surfaces were examined with atomic force microscopy (AFM), in air in contact- and non-contact mode, and a scanning electron microscope (SEM). The advantage of combining a tactile technique with an electron optical technique is that the tactile technique is very sensitive to the vertical scale yielding precise height measurements, while the electron optical methods are sensitive to the horizontal scale thus allowing precise width measurements. Energy-dispersive X-ray spectroscopy (EDXS) was employed for chemical analysis. All machines used for analysis are commercial instruments.

3 RESULTS

Evaporation of copper onto TiS_2 and WSe_2 lead to no special surface modification, only a dense layer of copper deposited on the crystal surface. This is in contrast to the observations made on VSe_2, TaS_2, and $TiTe_2$, in which the evaporated Cu atoms caused the formation of various surface structures. These are presented more detailed in the following sections.

3.1 Copper on VSe_2 in situ and ex situ

The results on the copper deposition onto VSe_2 in the low 10^{-10} mbar range reproduce results discussed earlier in [1]. Scanning tunneling microscopy and scanning electron microscopy reveal that the deposition Cu onto VSe_2 substrates in ultra-high vacuum leads to the self-organized formation of linear nanostructures, nanowires, and nanotunnels on the substrate surface. The nanowires and nanotunnels are approximately equiaxed and form networks with a mesh width several orders of magnitude larger than their diameter. Systematic increase of Cu coverage not only increases the thickness of the nanowires and nanotunnels but also induces the formation of further, distinct networks with increased diameter and increased mesh width. High Cu coverages, like the ones used here, lead to a hierarchy of apparently independent nanowire and nanotunnel networks on different length scales. No general difference can be found between the nanowire geometry observed in vacuum STM, air AFM and SEM, as shown in Figure 2.

Therefore, the VSe_2 crystals can be used as a reference sample for other TCMDs, ensuring that the different structures observed on other crystals are not a result of an altered preparation.

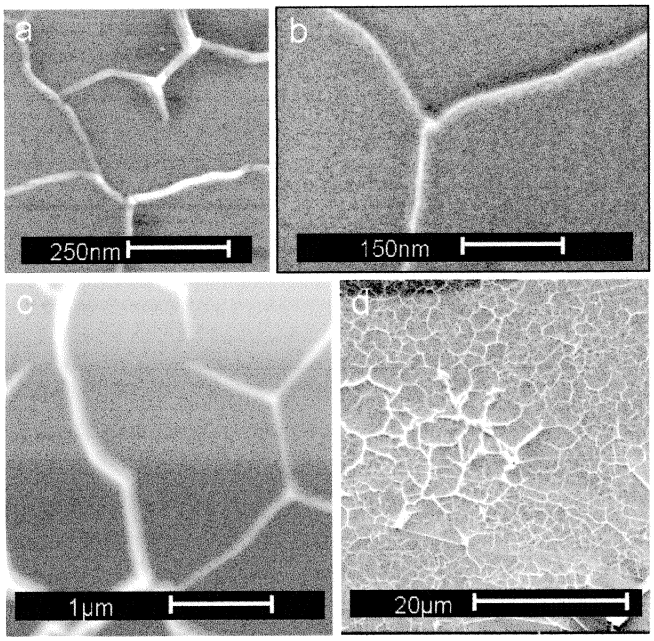

Figure 2: Different parts of nanowire networks obtain after copper evaporation on VSe_2. a) Vacuum STM image obtained directly after evaporation in vacuum. b) SEM image, obtained after transport through air. c) Air-AFM image in non contact mode. d) SEM overview image shows the entangled nature of the networks.

3.2 Copper on TaS_2

In contrast to the dense entangled nanowire networks found on VSe_2, on TaS_2, two different networks of relatively large nanotunnels and microtunnels can be found. They show structural similarity with the nanowire networks as they form also networks. But instead of nanowires they consist of tunnels and the dimensions, mesh width and tunnel diameter are a factor of 10-100 larger. These tunnels are also larger than the tunnels found among the nanowire networks on VSe_2. A similarity to the nanowires networks is the alignment of the tunnels. They are oriented only in three different directions. Type 1 of these tunnels is shown in Figure 3a. Large rings on the order of 5-30 µm are formed by these tunnels. The tunnel size of these Type 1 tunnels varies, from approximately 2µm at the middle to 3µm at the connection point of the tunnel. The tunnel character can be seen in images such as 3a, where the tunnel side is cracked open. The wall thickness of the tunnels is estimated to be less than 20 nm. The second type of tunnels is much smaller and is aligned more strictly, as in Figure 3b. There, the diameter of the tunnels is only 100nm while the separation distance is on the order of 10-100 µm.

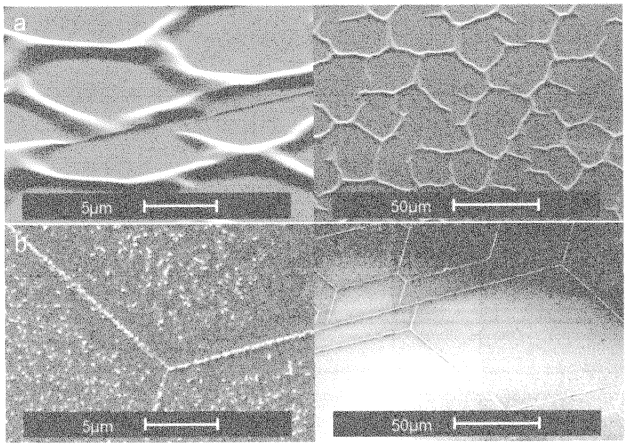

Figure 3: Different types of tunnel networks a) Type 1 of the tunnels shows a diameter around 1µm. mesh width is 5µm to 30µm. b) Tunnel networks of type 2 appear much more aligned. The tunnel diameter is smaller, around 100nm, but the mesh width is wider, ranging from 10µm to more than 100µm.

Hints for the diffusion process and growth mode of the copper on the flat surfaces can be obtained by performing an experiment creating a sharp step between an area that is exposed to copper and one which is copper free. Therefore one part of the crystal is shaded in a distance of approximately 50µm with a barrier preventing that copper will be deposited. The low distance over the surface ensures a sharp edge between the copper exposed and non-exposed area. Figure 4 shows that area where part A was exposed to copper and part B was shaded. Dendrite growth is visible, and dendrites reach into the area that was not exposed to copper. The largest dendrites can be found growing at some of the step edges. A closer look with higher magnification reveals a kind of pale shadow around the dendrites, shown in Figure 4.

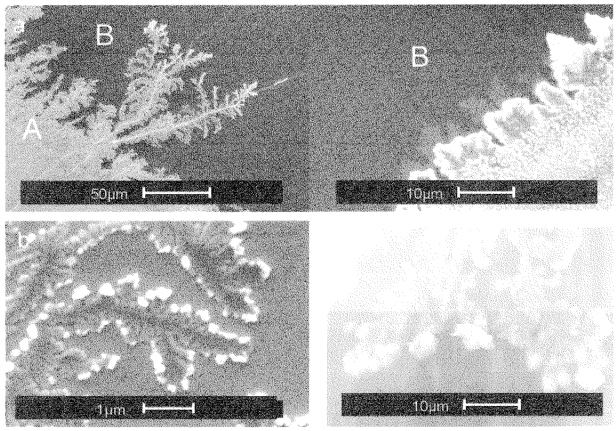

Figure 4: Dendrite shaped copper a) SEM overview shows dendrite growth at the edge between copper exposed area A and copper free area B. Left image shows a pale structure at the interface b) Magnification, the image on the right is an AFM image, giving the height scale.

These dendrites are surrounded by a structure with less contrast. In AFM it is evident that these areas are elevated approximately 10 nm above the pure layered crystal. EDX spectra reveal a similar amount of copper for the 10nm high areas and the dendrite body. Absolutely no copper can be detected in the area indicated by the arrows in 4b.

3.3 Copper on $TiTe_2$

No nanowires or tunnels could be found on the $TiTe_2$. Instead, the surface is covered with copper clusters, agglomerated to a film. Surprisingly, a long range order can also be found on some areas. Figure 5 shows an overview over an area which exhibits geometrical shapes formed by a lower cluster density.

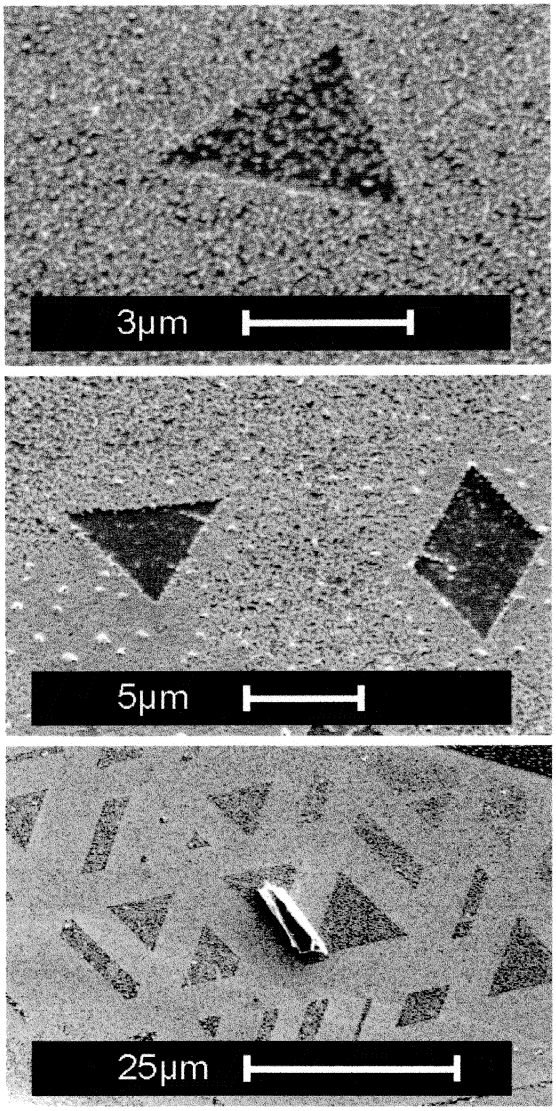

Figure 5: SEM images of copper clusters at different magnifications. Geometrical shapes like triangles or parallelograms can be found. The image in the middle shows that cluster density around the shapes is increased. (bottom image contains a dust particle)

The triangles, parallelograms, and other geometric shapes have a typical baseline width in the range of 1 μm to 10 μm. The lower cluster density in the structure obviously leads to a higher density on the outside. So coming from the outside to the inside of the structure the cluster density increases towards the structure, and than drops suddenly. Even if a shape completely different from wires and tunnels is formed, the structures show three orientation directions, forming a 120° angle similar to the nanostructures on VSe_2 or the tunnels on TaS_2.

4 DISCUSSION

In summary a wide variety of structures ranging from the nanoscale to the 100μm range can be found. This is quite unexpected, considering that the current textbook reasoning suggests that no structure would be found, especially not a structure with long-range order. The nanowire formation on the VSe_2 was explained by a charge transfer from the chemisorbed metal to the surface layers, resulting in a change in the lattice parameter in the quasi two dimensional surface layer. Finally, the stress leads to a structural failure in the surface layer, producing cracks into which the metal is physisorbed.

On the TaS_2 nearly no nanowires can be found. Therefore we assume that the charge transfer given by the copper layer leads only to compressive stress, which would be relaxed by the large tunnel structures. The appearance of only two reproducible different structures shows the interesting mechanics of the layered crystals. However, without clarifying these mechanical details, no interpretation can be found so far, since there is also no visible difference in the areas where one or the other type is located. Instead, it appears that they are distributed uniformly over the crystal. The appearance of the alignment is most likely induced by the crystal symmetry. The crystal can be deformed easier in certain crystallographic directions, which are more sensitive to a structural breakdown.

The large fractal-shaped clusters at the edge between the copper exposed and the pure surface are obviously due to a diffusion limited aggregation (DLA) growth process because of the similarity in the geometric appearance. Yet, the setup here is different from the usual setup where this type of growth can be observed. A suggested explanation could be as follows: Copper arrives on the TaS_2 surface. Atoms diffuse around forming a nucleation site when they collide with each other. However, fewer Cu atoms will diffuse into the shaded area, resulting in a low probability of collisions and thus nucleation. Nonetheless, nucleation will occur if they return during their random walk to the edge or if they collide with a step edge. This shows that the diffusion length must be extremely long, at least in the order of the large dendrite length, which is 50μm. The EDX proves that there is almost no copper in the covered area. Comparing the sensitivity of the EDX at the 10nm thick area with the spectra obtained in the uncovered area, there must be a maximum of less than a monolayer of copper. In addition, no surface elevations could be found by AFM.

The most unusual features are the formation of the geometrical shaped areas. The only hint to their origin is the threefold symmetry of their borders. However, a simple stress explanation, as in the case of the wires, cannot explain this phenomenon. No defects could be found on this scale, but we can not exclude a slight change in crystal structure in the shapes. But even if a defect would be assumed, the behaviour is total different from a usual material agglomeration at a defect.

All these structures observed here show that the very flat structureless surfaces are surprisingly well-suited for self-organized growth of nanostructures and microstructures. This is partly due to stress induction in the substrate. The stress has a more pronounced effect on structureless surfaces than on structured ones, where other effects dominate. An additional advantage of a flat, non-reactive substrate is the long diffusion length (usually the barrier for atomic hopping can be overcome at room temperature) and the weak bonding to the substrate, allowing a rearrangement of obtained structures thereby amplifying the self-organization processes.

5 ACKNOWLEDGEMENTS

The authors would like to thank Prof. Faupel for providing his laboratory and fruitful discussion and Whitney Hartung for help on preparing this manuscript. Financial support was given by the DFG, Forschergruppe Project FOR 353/2-1.

REFERENCES

[1] R. Adelung, F. Ernst, A. Scott, M. Tabib-Azar, L. Kipp, M. Skibowski, S. Hollensteiner, E. Spiecker, W. Jäger, S. Gunst, A. Klein, W. Jägermann, V. Zaporojtchenko, F. Faupel, Adv. Mater. 15, 1056, 2002.

[2] J. Wilson and A. Yoffe, Adv. Phys. 18, 193, 1969.

[3] M.S. Whittingham, Science 192, 1126, 1976.

[4] G. Prasad and O. Srivastava, J. Phys. D **21**, 1028, 1988.

[5] W. Jaegermann, Surface Studies of Layered Materials in Relation to Energy Converting Interfaces, Vol. 14 of Physics and Chemistry of Materials with Low-Dimensional Structures: Photoelectrochemistry and Photovoltaics of Layered Semiconductors, Kluwer Academic, Dordrecht, p. 195, 1992.

[6] R. Adelung, J. Brandt, K. Roßnagel, O. Seifarth, L. Kipp, M. Skibowski, C. Ramirez, T. Strasser, and W. Schattke, Phys. Rev. Lett. 86, 1303, 2001.

[7] R. Adelung, J. Brandt, L. Kipp and M. Skibowski, Phys. Rev. B. 63, 165327, 2001.

[8] J. Viernow, J.-L. Lin, D. Y. Petrovykh, F. M. Leibsle, F. K. Men, and F. J. Himpsel, Appl. Phys. Lett. 72, 948 (1998).